Lung MRI scoring reveals persistence of emphysema-like changes in lungs of infants born preterm at (pre)school age

Kai Förster[1,2,3,12], Kathrin Strobl[1,12], Alida Kindt[4,12], Friederike Häfner[1,3], Benjamin Schubert[5,6], Florian Heinen[1,7], Andreas W. Flemmer[2], Denise Steffinger[8], Olaf Dietrich[8], Sophia Stoecklein[8], Folke Brinkmann[9,10] and Anne Hilgendorff[1,3,11]

[1]Dr. v. Hauner University Children's Hospital, LMU Hospital, Munich, Germany. [2]Division Neonatology, Dr. v. Hauner University Children's Hospital, LMU Hospital, Munich, Germany. [3]Comprehensive Pneumology Center, Helmholtz Zentrum München, Member of the German Lung Research Center (DZL), Munich, Germany. [4]Metabolomics and Analytics Centre, Leiden Academic Centre for Drug Research (LACDR), Leiden University, Leiden, The Netherlands. [5]Institute of Computational Biology, Helmholtz Zentrum München, Munich, Germany. [6]Department of Mathematics, Technische Universität München, Garching, Germany. [7]Department of Pediatric Neurology, Dr. v. Hauner University Children's Hospital, LMU Hospital, Munich, Germany. [8]Department of Radiology, LMU University Hospital, LMU Munich, Munich, Germany. [9]Department of Pediatric Pneumology and Allergology, University Hospital Schleswig-Holstein UKSH, Campus Lübeck, Lübeck, Germany. [10]Airway Research Center North (ARCN), Germany, Member of the German Center for Lung Research (DZL), Munich, Germany. [11]School of Medicine and Health Sciences, Department of Paediatrics, Section of Neonatology, Pediatric Intensive Care, Pediatric Cardiology, Pediatric Pneumology and Allergology and Research Centre Neurosensory Science, Carl von Ossietzky University Oldenburg, Oldenburg, Germany. [12]The first three authors contributed equally to the study.

Corresponding author: Anne Hilgendorff (anne.hilgendorff@uni-oldenburg.de)

Shareable abstract (@ERSpublications)
Lung MRI revealed emphysema-like changes at (pre)school age in moderate/severe BPD. These changes were associated with the degree of immaturity at birth and coincided with indicators of airway pathology. Such structural information is needed to inform long-term treatment and monitoring strategies. https://bit.ly/44nNj9W

Cite this article as: Förster K, Strobl K, Kindt A, *et al*. Lung MRI scoring reveals persistence of emphysema-like changes in lungs of infants born preterm at (pre)school age. *ERJ Open Res* 2025; 11: 01183-2024 [DOI: 10.1183/23120541.01183-2024].

This article has an editorial commentary: https://doi.org/10.1183/23120541.00528-2025

Received: 11 Nov 2024
Accepted: 6 April 2025

Abstract

Background Chronic lung disease, *i.e.*, bronchopulmonary dysplasia (BPD), is the most prevalent complication after premature birth. Despite the clinical relevance, insight into persisting lung structural changes in BPD in later childhood remains sparse. We therefore assessed lung structural changes by magnetic resonance imaging (MRI) in (pre)school-aged children born before 32 weeks' gestation and compared them to pulmonary characteristics of BPD at near-term age.

Methods (Pre)school-aged children after premature birth with and without BPD underwent 3T MRI without sedation at a median age of 5.8 years (4.3–8.7 years, n=27). Comparative analyses used imaging at near-term age in 88 preterm infants with a subgroup of 16 serial measurements. Standardised image analysis (consensus panel scoring, 5-point Likert scale) of coronal/axial/sagittal T2-weighted single-shot fast-spin-echo sequences obtained scores for the variables "emphysema", "interstitial enhancement", "airway accentuation" and "ventilation inhomogeneity", complemented by transverse (T2) and longitudinal (T1) relaxation-time mapping (n=26), lung volume measurements and follow-up parental questionnaires.

Results MRI scoring revealed persisting emphysema-like changes in children with moderate/severe BPD (p=0.031 *versus* no BPD). The prevalence was associated with greater immaturity (p=0.018) and in line with an increase in lung volume. In contrast, higher scores for "interstitial enhancement" and "airway accentuation" were not associated with a history of BPD at (pre)school age.

Interpretation Persisting structural changes in the BPD lung are dominated by underlying immaturity and demonstrate an emphysema-like phenotype, potentially fitting the concept of dysanapsis. Lung MRI can inform treatment and monitoring strategies through the provision of additional information on disease characteristics and severity.

Introduction

With the continuous improvement of medical care for premature infants, the probability of survival has increased particularly for very premature newborns [1, 2]. However, these children face a significant risk for long-term complications [3–6] such as neonatal chronic lung disease, also known as bronchopulmonary dysplasia (BPD) [7]. This most prevalent morbidity after premature birth results from the exposure of the functionally and structurally immature lungs to postnatal challenges including mechanical ventilation and supplemental oxygen, adding to the detrimental effects of pre- and postnatal infections and malnutrition [8]. The concert of these risk factors lead to the disruption of alveolar and vascular formation as well as interstitial remodeling, critically reducing the functional capacity of the gas exchange area [7, 9].

Follow-up studies have indicated severe long-term pulmonary impairment as a consequence of prematurity [10, 11], supported by lung function studies in school age showing persistent deficits in baseline lung function [12]. The increased rate of sudden cardiac death observed in Scandinavian epidemiological studies confirms the significant prevalence for cardiopulmonary morbidity in this patient cohort [13, 14].

Despite the long-term clinical relevance of the disease, information about structural and functional pulmonary development is sparse and its assessment is not routinely integrated into the diagnostic process, thereby withholding critical information from individualised monitoring and treatment strategies.

As of today, lung imaging for respiratory distress is confined to conventional chest radiography (CXR) in the preterm infant, mainly due to the lack of alternative strategies. The diagnostic value of CXR, however, is limited due to its low sensitivity and specificity to identify structural changes [15], resulting in the failed success of implementing CXR-based scores into clinical routine [16]. Nevertheless, studies using CXR confirmed BPD characteristics in infants with oxygen dependency at 1 month of age including fibrosis/interstitial shadows, cystic elements and hyperinflation [17], later successfully correlating these findings with prolonged ventilator and oxygen dependency as well as abnormal airway resistance at 6 months of age [18]. Although computed tomography (CT) as the diagnostic alternative would benefit from high spatial resolution and improved diagnostic accuracy, its clinical application is limited due to radiation exposure [19–22].

With the ultimate aim to close the resulting diagnostic gap with a radiation-free, sensitive imaging tool, the neonatal community acknowledged the technical advances made in magnetic resonance imaging (MRI) [23–25] that had led to the successful application of this technique in adult and paediatric lung disease patients, even demonstrating comparability to high-resolution CT-derived structural information [26–28].

To evaluate the potential of the lung MRI-based disease score as a radiation-free, clinically applicable method to characterise structural abnormalities in BPD, we performed a follow-up study of the AIRR (Attention to Infants @ Respiratory Risk) cohort that included preterm infants born before 32 weeks gestational age (GA) at (pre)school age and quantified the extent of the observed lung structural changes. This follow-up study enabled us to highlight the predominance of tissue rarefication and overdistension resembling emphysema-like structural changes in the lungs of (pre)school-aged children with BPD, more prevalent in infants born with significant immaturity and associated with structural airway abnormalities and increased MRI lung volumes.

Methods

Patient recruitment

Preterm infants ⩽32 weeks GA born at the Perinatal Center of the Ludwig-Maximilian University, Campus Großhadern between 2013 and 2018 with and without BPD were prospectively included in the study after written informed parental consent (EC #195-07, Ethic Board of the Ludwig-Maximilians University, German Registry for Clinical Studies DRKS00004600). Severe congenital malformations (*e.g.*, hypoplastic left-heart syndrome, severe hypoplasia of the lungs or congenital diaphragmatic hernia (CHD)), chromosomal abnormalities (*e.g.*, trisomy 13 or 18), inborn errors of metabolism, and decision for palliative therapy directly after birth resulted in exclusion from the study.

Follow-up studies in the AIRR cohort were performed between April 2018 and May 2022 to re-recruit children between the age of 4 and 8 years. The AIRR cohort comprised patients with (n=97) and without (n=96) MRI at near-term age. Out of 97 patients of the AIRR study with MRI at near-term age, 79 children were at an appropriate age for MRI at (pre)school age during this time. Of these, a total of 13 could not be reached *via* phone or mail. Of the remaining 66 families, 26 families were willing to perform a second MRI. In two families travel to the study site was too demanding, and in four cases comorbidity development in the child would have required sedation to perform the MRI, resulting in a total of 20 cases

for MRI at (pre)school age. From the MRIs performed, four cases were unsuccessful due to non-compliance in the scanner, resulting in a total of 16 cases in which an MRI was performed in the neonatal period and at (pre)school age. From the 96 patients of the AIRR study without an MRI at near-term age, 61 children were at an appropriate age for MRI during this time. A total of 15 could not be reached *via* phone or mail. Of the remaining 46 families, 11 were willing to perform an MRI at (pre)school age. In total, MRI studies were available from 27 children at (pre)school age (table 1). MRI at near-term age was available for 88 cases with nine cases excluded due to poor imaging quality.

Patient characterisation

The clinical course from birth to discharge was comprehensively monitored in all study infants as published previously [29] using the following consented definitions – intrauterine growth restriction: birthweight below the 10th percentile; diagnosis and severity of respiratory distress syndrome (RDS): assessment of anterior–posterior chest radiographs according to Couchard *et al.* [30]; chorioamnionitis: inflammatory alterations of the chorionic plate (histological examination) or signs of maternal and fetal infection [31]; presence of early postnatal systemic infections (early-onset infection): one or more clinical and laboratory sign of infection according to Sherman *et al.* [32]. BPD was defined according to the NICHD/NHLBI/ORD workshop [7] based on the need for oxygen supplementation (inspiratory oxygen fraction (F_{IO_2}) >0.21) for at least 28 days, followed by a final assessment at 36 weeks postmenstrual age (PMA) or at discharge, whichever came first in preterm infants born at <32 weeks GA. Study infants were accordingly assigned as having mild BPD (requirement of supplemental oxygen for 28 days, no need for oxygen supplementation at 36 weeks PMA) or moderate BPD (oxygen supplementation F_{IO_2} <0.30 at 36 weeks PMA), and severe BPD (oxygen supplementation F_{IO_2} >0.30 at 36 weeks PMA and/or positive pressure ventilation/continuous positive pressure) with each treatment referring to its continuous application and oxygen supplementation >12 h equaling 1 day of treatment. The infants' oxygen saturation was assessed by standardised pulse oximetry. No infant was discharged from hospital before 36 weeks' gestation. At the time of MRI none of the children received treatment with diuretics or steroids and none of the infants presented with a haemodynamically relevant persistent ductus arteriosus. BPD incidences and comorbidities are indicated in table 1.

TABLE 1 Patient characteristics

Clinical variables	Total	No BPD	Mild BPD	Moderate/severe BPD
Patients, n	27	8	10	9
Gestational age at birth weeks#	26.4 (23.5–31.4)	29.5 (26.5–31.4)	25.8 (23.5–30.4)	25.3 (24.0–28.4)
Age at follow-up MRI years	5.8 (4.3–8.7)	5.7 (4.3–7.2)	6.4 (4.7–7.7)	5.5 (4.7–8.7)
Birthweight g#	920 (300–1560)	1270 (960–1350)	850 (540–1560)	670 (300–925)
Sex (female/male)	12/15 (44.4%/55.6%)	4/4 (50.0%/50.0%)	4/6 (40.0%/60.0%)	4/5 (44.4%/55.6%)
Antenatal corticosteroids (yes/no)	22/4 (84.6%/15.4%)	7/1 (87.5%/12.5%)	8/1 (88.9%/11.1%)	7/2 (77.8%/22.2%)
Postnatal corticosteroids (yes/no)#	13/14 (48.1%/51.9%)	2/6 (25.0%/75.0%)	3/7 (30.0%/70.0%)	8/1 (88.9%/11.1%)
Neonatal intensive care unit stay days	79 (21–150)	51 (21–123)	79 (31–110)	107 (65–150)
Early onset infection (yes/no)#	12/15 (44.4%/55.6%)	0/8 (0%/100%)	8/2 (80.0%/20.0%)	4/5 (44.4%/55.6%)
ROP grade ⩾3 (yes/no)	6/21 (22.2%/77.8%)	1/7 (12.5%/87.5%)	2/8 (20.0%/80.0%)	3/6 (33.3%/66.7%)
RDS grade ⩾3 (yes/no)	10/17 (37.0%/63.0%)	2/6 (25.0%/75.0%)	5/5 (50.0%/50.0%)	3/6 (33.3%/66.7%)
IPPV (days) or mechanical ventilation#	13 (0–46)	0 (0–2)	13 (0–38)	27 (1–46)
NIPPV (days) or CPAP (days)#	44 (5–102)	25 (5–34)	50 (13–72)	53 (34–102)
IUGR (yes/no)	7/20 (26.0%/74.0%)	2/6 (25.0%/75.0%)	3/7 (30.0%/70.0%)	2/7 (22.2%/77.8%)
Chorioamnionitis (yes/no)	10/17 (37.0%/62.0%)	3/5 (37.5%/62.5%)	5/5 (50.0%/50.0%)	2/7 (22.2%/77.8%)
Oxygen supplementation required (yes/no)	26/1 (96.3%/3.7%)	7/1 (87.5%/12.5%)	10/0 (100.0%/0.0%)	9/0 (100.0%/0.0%)
Oxygen supplementation days#	47.5 (0–129)	3.5 (0–27)	49 (20–90)	111 (46–129)

Clinical characteristics for all patients (n=27) were included. Values are median (range) or n (%). BPD was graded according to the definition of Jobe and Bancalari [7]: mild (oxygen supplementation for at least 28 days postnatally), moderate (oxygen supplementation <30% at 36 weeks postmenstrual age) and severe (oxygen supplementation >30% and/or ventilator support at 36 weeks postmenstrual age). Systemic infections were diagnosed according to Sherman *et al.* [32] based on one or more clinical and laboratory signs of infection. Postnatally, diagnosis and severity of RDS were scored on anterior–posterior chest radiographs according to Couchard *et al.* [30]. Intrauterine growth restriction (IUGR) was defined as birthweight below the 10th percentile. Chorioamnionitis was defined as inflammatory alterations of the chorionic plate (histological examination) or signs of maternal and fetal infection [31]. BPD: bronchopulmonary dysplasia; MRI: magnetic resonance imaging; ROP: retinopathy of prematurity; RDS: respiratory distress syndrome; IPPV: invasive positive pressure ventilation; NIPPV: noninvasive positive pressure ventilation; CPAP: continuous positive airway pressure. p-values were calculated using Fisher's exact test and ANOVA for categorical and continuous variables, respectively. #: p<0.05.

Magnetic resonance imaging

Pulmonary MRI

(Pre)school-aged children after premature birth underwent 3 tesla (3T) MRI at a median age of 5.8 years (4.3–8.7 years, n=27). Serial measurements referring to cases with MRI measurements at near-term and at (pre)school age were acquired in 16 cases. Initial MRI at the time of the BPD diagnosis was acquired in 88 infants as reported previously [33].

No CXRs, due to its limited value to inform treatment decisions in routine follow-up care for BPD [15], or CT scans, due to radiation exposure [22], were available at the time of MRI for comparison.

Imaging protocol

Lung MRI was performed in unsedated (pre)school-aged children, awake or in spontaneous sleep in supine position using a 3T whole-body MRI scanner (Magnetom Skyra, Siemens Healthineers, Erlangen, Germany). Noise attenuators were used for hearing protection. MRI was performed with a size-adapted number of coil elements from the 32-channel spine array coil, an 18-channel flexible body array coil and a 20-channel head-and-neck array coil. The protocol included pulse sequences for the qualitative and quantitative assessment of morphology, volume and structural changes of the lung. In detail, the following pulse sequences were used for the scoring study: T2-weighted single-shot fast-spin-echo (Half-Fourier-Acquired Single-shot Turbo spin Echo, HASTE) sequences in coronal and axial (voxel size $1.3\times1.3\times4.0$ mm^3) as well as in sagittal orientations (voxel size $1.2\times1.2\times4.0$ mm^3). Echo time (TE) was 57 ms. Acquisitions were ECG-triggered with a minimum repetition time (TR) of two R-R intervals; two signal averages were acquired. Parallel imaging with an acceleration factor of two was used. In coronal and axial orientation, about 30 slices with a field of view (FOV) of 340×255 mm^2 and a resolution of 256×192 pixels were acquired. In sagittal orientation, about 40 slices with a FOV of 300×197 mm^2 and a resolution of 256×168 pixels were acquired. FOV and slice number were individually adjusted to the size of the participants. The scan durations of the T2-weighted HASTE sequences varied depending on the cardiac frequency. Typical scan durations were between 40 s and 120 s for each of the three (coronal, axial and sagittal) acquisitions.

For comparison, MR images were available from unsedated, spontaneously breathing infants at near-term age swaddled in a vacuum mattress after feeding as described previously [33] following the identical size-adjusted imaging protocol described above.

Image analysis

Pre-scoring for image quality and scoring of the T2-weighted single-shot fast-spin-echo sequences was performed by a consensus panel (two neonatologists, 15 years of professional experience trained by a senior radiologist with >20 years of professional experience and a fifth-year medical student), resulting in consortial agreement. The reader-based image assessment was performed blinded to the clinical information using dedicated medical-imaging monitors certified for radiological reading and diagnostic purposes [33].

All images had to fulfil the following quality criteria: symmetrical visualisation of the thorax, the clavicles, and the ribs; visualisation of the spine and the paraspinal structures; visual discrimination of the cervical and thoracic trachea, their bifurcation and the central bronchi; visualisation of the costo-pleural border from the apex of the lung to the diaphragmatic-rib angle; visual discrimination of the hilar, the heart and diaphragm; visualisation of vascular drawing in the lung core; visual discrimination of vessels possibly down to the lung periphery; avoidance of superimposition of the upper fields by the scapulae; and visualisation of the thymus. Prescoring of all images included the following criteria: 1) assessment of technical image quality including motion artefacts, imaging artefacts and a low signal-to-noise ratio; 2) presence of complications, *i.e.*, infiltrates, pneumothorax or pleural effusion; 3) assessment of inflation levels (1 (normal), 2 (overdistended), 3 (underinflated)) describing extremes of the ventilation situation during imaging to establish standardised conditions for the subsequent analysis. Insufficient technical image quality and/or presence of one complication and/or presence of “overdistension” or “underinflation” resulted in the exclusion of the MRI scan from analysis.

Morphological MRI score

Standardised image analysis addressed structural changes of the BPD lung described by previous CT and MRI studies [19, 20, 22, 34] using the following variables in a score based on a 5-point Likert scale as published previously [33]: “emphysema”, “interstitial enhancement” and “airway accentuation” indicating remodeling of the lung scaffold including the bronchial tree next to the presence of caudo-cranial and anterior-to-posterior gradients of signal intensities reflecting “ventilation inhomogeneity”. Scoring

parameters were defined as follows: “emphysema” was reflected by reduced signal intensity, rarefied lung vasculature, hyperexpansion, mosaic pattern of lung attenuation, presence of bullae or blebs; “interstitial enhancement” was reflected by distinctive representation of interstitial structures, thickening of broncho-vascular bundles; “airway accentuation” was reflected by increased signal intensity in the respiratory ducts and scored based on airway wall thickness in relation to airway diameter; differences in signal intensities (caudo-cranial as well as anterior-to-posterior) over all lung quadrants were summarised in the variable “ventilation inhomogeneity”. On a semi-quantitative five-point Likert scale [35] a score of “1” represented the absence of any abnormality, while a score of “5” represented maximum pathology. To achieve a high level of standardisation, we virtually segmented the lung into four quadrants (upper left, upper right, lower left and lower right quadrants) based on the dimensions of the lung scan. Scoring was performed separately for each variable for the right and left lung (each for the upper and lower quadrant) and in coronal and axial as well as in sagittal images to allow for the detection of regional differences [33, 35].

T1/T2 relaxation times

For T1-mapping/T2-mapping analysis ECG-triggered T1/T2-weighted single-slice fast spin echo sequences were used (n=26). Manual segmentation of the lungs in the acquired slice was performed with the ITK-SNAP software (version 3.8.0). T1 and T2 relaxation times maps were calculated pixel-by-pixel by nonlinear exponential signal fitting using kmpfit from the python-based Kapteyn package. Median value and interquartile ranges of T1 and T2 were determined over all lung pixels of each participant.

Lung volume

Transversal T2-weighted single-shot fast-spin-echo sequences were used for manual lung segmentation in ITK-SNAP. The annotations of each slice were used to reconstruct a three-dimensional mask of the lung followed by lung volume calculation.

Parental assessment of pulmonary outcome parameters

A short parental questionnaire asked for information about acute and chronic respiratory infections and diseases after discharge from neonatal care, and hospitalisation rates as well as use of medication. The questionnaire was provided to 120 families by mail or at the time of MRI following written informed consent. Of the 27 children examined, 16 questionnaires were available for analysis. The questionnaire was completed by the mother, the father or both parents.

Data analysis

Differences of continuous variables were assessed by Mann–Whitney U-test when investigating MRI scores and T1/T2 relaxation times, while t-test was applied when investigating birthweight. Discrete variables were assessed using a Fisher’s exact test. Near-term and (pre)school measurements were treated independently. The data were stratified by GA (⩽28/>28 weeks) to investigate short and long-term effects of this established risk factor for pulmonary morbidity in children after premature birth. The median of the interstitial enhancement score and the emphysematous changes were used to further stratify the cohort and investigate differences in clinical variables associated with extreme scores. Multivariate regression models were calculated to associate immaturity (⩽28/>28 weeks) with scores accounting for days of invasive and noninvasive mechanical ventilation, postnatal steroid medication (yes/no) and sex. For differences observed in the patients’ characteristics the Fisher’s exact test and ANOVA for categorical and continuous variables were applied, respectively.

In line with previous studies and in order to adequately account for the impact of prematurity, preterm infants without BPD were used as control cases [23, 24]. No significant differences were observed regarding age at MRI, sex, use of antenatal corticosteroids, incidence of intrauterine growth retardation, chorioamnionitis, frequency or severity of RDS, incidence or severity of ROP or duration of neonatal intensive care unit stay between the group of infants with and without BPD. Given the prevalent risk factors for BPD, differences were observed for gestational age, birthweight, use of postnatal corticosteroids, frequency of early onset of infection, duration of mechanical ventilation (invasive and noninvasive positive pressure ventilation) as well as duration of oxygen supplementation between the two groups.

Results

At (pre)school age, MRI studies were available from 27 children (table 1). For comparative analysis, MRI performed at near-term age was available for 88 infants [33]. Findings were obtained by MRI-based consensus scoring on a five-point Likert scale using T2-weighted single-shot fast-spin-echo sequences.

Emphysema-like changes dominate lung structural abnormalities in MRI in (pre)school-aged children after premature birth with severity depending on lung disease and degree of immaturity

Lung structure in preterm infants born <32 weeks GA that were diagnosed with moderate and severe BPD at 36 weeks PMA was dominated by changes resembling emphysema when reaching (pre)school age as compared to infants with no or mild BPD (p=0.015) or mild BPD (p=0.03; figure 1a), thereby confirming structural changes observed at near-term age. The changes were significantly associated with the degree of immaturity at birth, again in line with results near-term [33] that demonstrated a predominance of tissue rarefication and overdistension, summarised as emphysema-like changes to the lung structure in infants born ⩽28 weeks GA (p=0.02) (figure 1b). A multivariate model considering immaturity (⩽28/>28 weeks GA), noninvasive and invasive mechanical ventilation duration (days), sex and postnatal steroid treatment showed an association of invasive mechanical ventilation in the postnatal period with tissue rarefication and overdistension in (pre)school children (estimate= −0.05; p=0.075). In serial analyses, a persistence of these emphysema-like changes was found in 50% (n=7) of all children at (pre)school age. Infants with consistently high or increased scores for the variable previously described as "emphysema" [33] at (pre) school age were characterised by elevated scores for "airway accentuation (r=0.68, p=0.0074) (figure 1c). In contrast, the elevated scores for the variable "emphysema" [33] at (pre)school age were negatively correlated with T1 relaxation, thereby recapitulating previous observations at near-term age [33, 36–38] where decreased T1 relaxation times were interpreted as a proxy of emphysema-like structural changes (r= −0.35, p=8×10^{-2}) (figure 1d) [37, 39]. In line with these findings, we detected a 17% increase in lung volume as assessed by MRI in children with BPD (mean volume no BPD: 596.45 cm^3; mean volume BPD: 696.61 cm^3; p=9.8×10^{-2}, figure 2).

In contrast, lung MRI at (pre)school age did not demonstrate an increase in "interstitial enhancement" in infants with moderate/severe BPD (p=4.6×10^{-1}) (figure 3a) or associations of this score with degree of immaturity (p=9.0×10^{-2}) (figure 3b), thereby in contrast to the results obtained in infants with BPD at near-term age (p=2.7×10^{-3}) (figure 3a,b) [33]. In 50% of the cases (n=7), however, elevated scores for "interstitial enhancement" persisted into (pre)school age when complementing group comparisons by serial analysis. In line with the findings obtained by scoring, T2 relaxation times were not found to differ across BPD grades (no BPD *versus* mild BPD: p=4.6×10^{-1}; no BPD *versus* moderate/severe BPD: p=5.1×10^{-1}; mild BPD *versus* moderate/severe BPD: p=9.7×10^{-1}; Mann–Whitney U-test).

Airway accentuation was observed to characterise infants with mild BPD at (pre)school age (p=5.0×10^{-2}) (figure 3c), together with an impact of the degree of immaturity (p=6.60×10^{-3}) (figure 3d). In contrast, MRI at near-term age demonstrated an increase in "airway accentuation in infants with moderate/severe BPD (p=3.8×10^{-2}) while no impact of GA was observed (p=2.6×10^{-1}) (figure 3c,d).

Analysis of the data provided by the parental questionnaire did not reveal a significant correlation with the reported rates of respiratory infections and the scores obtained for the variables described as "airway accentuation" or "emphysema" at (pre)school age. A subanalysis for the variables "asthma" or "bronchitis" could not be performed due to data missingness.

Figure 4 provides exemplary MRI images of infants with elevated and non-elevated scores for the variables assessed.

Discussion

To characterise structural and functional changes in BPD as a critical prerequisite to inform individual monitoring and treatment strategies, we utilised 3T lung MRI and identified persisting structural changes reflecting tissue rarefication and overdistension (here summarised in the variable "emphysema") in preterm infants with BPD at (pre)school age. The changes were supported by increased MRI lung volumes and were found to be most pronounced in infants with greater immaturity at birth. Our findings are reflected by imaging and lung function studies that detected lung structural abnormalities at the age of 5–12 years in up to 90% of patients with BPD [40–45]. In line with our results, the extensive structural abnormalities observed in other studies were not only related to BPD, but demonstrated a strong relation to the degree of prematurity [43], mirrored by changes to lung function [44]. Many studies, however, demonstrated an overlapping association with the history of postnatal oxygen supplementation and mechanical ventilation [45–47].

In contrast to the persistence of tissue rarefication and overdistension described as emphysema-like changes into (pre)school age, differences that reflect interstitial remodeling and/or oedema were not observed at this later time point, despite their presence at near-term age as identified by us and others [33, 48]. This phenomenon was already described by studies that used CT imaging, where the size and number of pulmonary opacities was found to decrease with maturation [49].

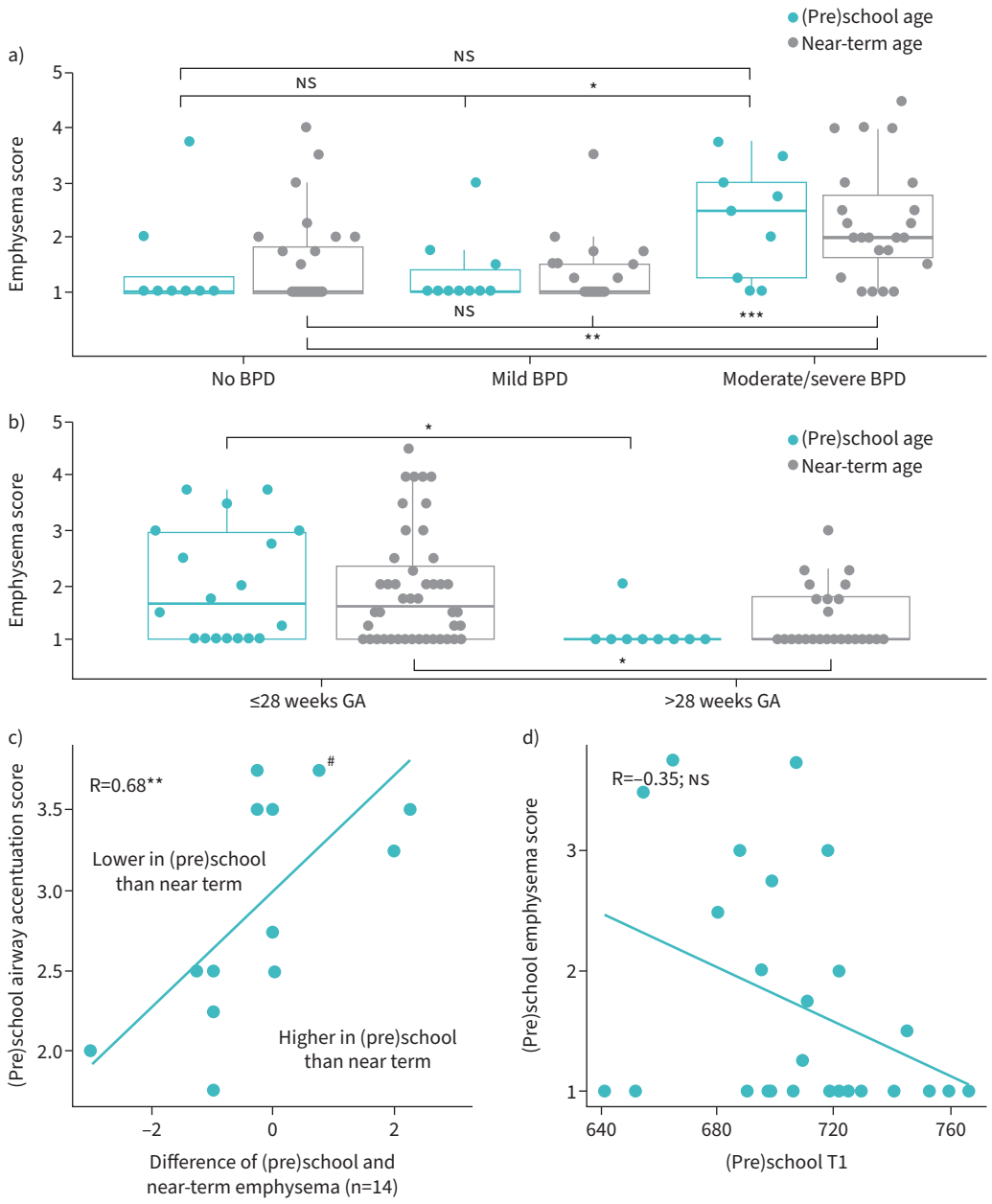

FIGURE 1 a) Increased scores for the variable "emphysema" [33] in preterm infants with moderate/severe bronchopulmonary dysplasia (BPD) at (pre)school and near-term age when compared to infants without or with mild BPD. b) Increased scores for "emphysema" in preterm infants born ⩽28 weeks gestational age (GA) at (pre)school and near-term age when compared to infants born >28 weeks GA. c) Positive correlation of identically elevated or increased scores for the variable "emphysema" at (pre)school age with heightened scores for the variable "airway accentuation" at (pre)school age. #: two overlapping dots. d) Spearman correlation between emphysema scores and T1 values at (pre)school age. The MRI score is based on a semi-quantitative 5-point Likert scale, where 1 represents the absence of any abnormality, 5 represents maximum pathology. Median, 25% and 75% quartiles; whiskers represent 1.5 times the interquartile range (IQR). NS: nonsignificant. NS: p>0.05; *: p⩽0.05; **: p⩽0.01; ***: p⩽0.001. In boxplots, p-values were calculated by Mann–Whitney U-test.

The fundamental changes in lung structure and function during development in the first decade of life [20, 49–51], including ongoing alveolar differentiation through developing and refining secondary septa and the capillary bed, may (partially) ameliorate interstitial changes observed early after birth. The "tissue deficit", however, likely persists as a result of the mismatch between structural and organ growth [52], individually

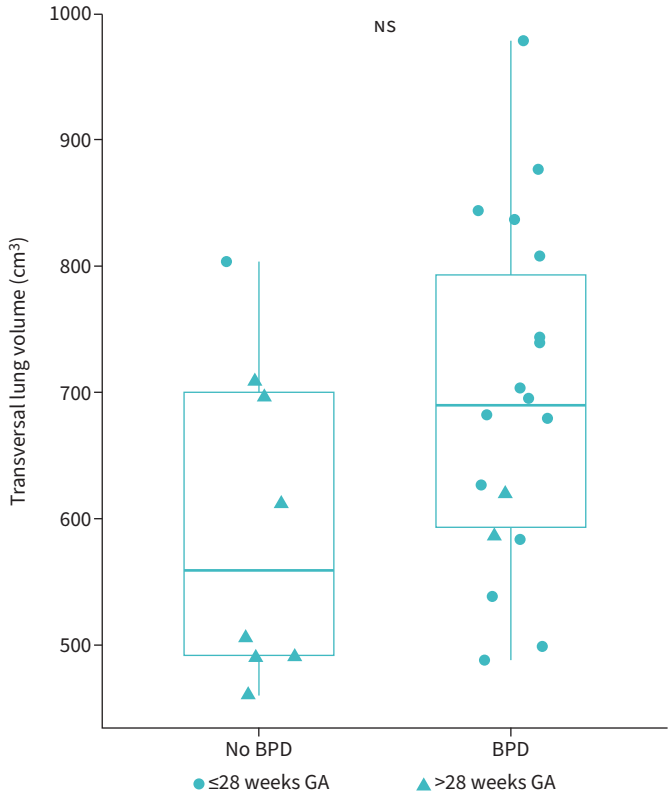

FIGURE 2 Assessment of (pre)school lung volume (cm^3) from transversal lung annotation with bronchopulmonary dysplasia (BPD). Points indicate individual cases. Median, 25% and 75% quartiles; whiskers represent 1.5 times the interquartile range (IQR). t-test p=0.092. NS: nonsignificant.

aggravated by non-optimal nutrient supply, inflammation and oxidative stress [53, 54], acting beyond the background of (mostly unidentified) (epi-)genetic factors [55–57]. The initial rarefaction of the gas exchange area [58] and the subsequent lack of catch-up growth [46, 47, 59, 60] is mirrored by the clinical presentation of BPD [61–66], leading to an early decline in lung function with aging [67]. Technically, the predominance of structural changes with tissue rarefication and overdistension attributed to the variable "emphysema" could be (partially) explained by a "halo effect" where MRI signal voids reflect abnormally enlarged terminal airspaces caused by truncated alveolarisation following prematurity. Further, the "overshadowing" of the emphysema-related signal in relation to the signal induced by interstitial thickening might reflect the reduction in blood flow and vascularisation [68].

The association between the structural abnormalities with emphysema-like changes and indications of airway remodeling observed by our study is well in line with clinical presentation and lung function measurements obtained in BPD patients. Measurements of pulmonary function by body plethysmography, mostly restricted to assessments in (pre)school age by specialised centres, indicate signs of airway obstruction associated with wheezing and other respiratory symptoms leading to the need for treatment in the first year of life [69, 70]. These changes are partnered with increased functional residual capacity in infants with BPD [71], resulting in lung dysfunction in older children and adults with BPD with airflow limitation, air trapping and lung hyperinflation [72–74].

The outlined picture of lung function abnormalities and histopathological changes in BPD [75], demonstrating persistent abnormalities in central and small airways together with a marked reduction in alveolarisation and vascular growth [76–78], fits the concept of "dysanapsis", describing the disrupted coordination of airway and parenchymal growth that results in a mismatch in airway-parenchymal-size relations. The concept, based on a spirometric pattern of a reduced forced expiratory volume in 1s/forced vital capacity ratio [79, 80], accompanied by structural changes in lung imaging [81], relates airflow limitations in early life to adulthood disease [82, 83]. Likely linked to gen- and exposomics [80], the

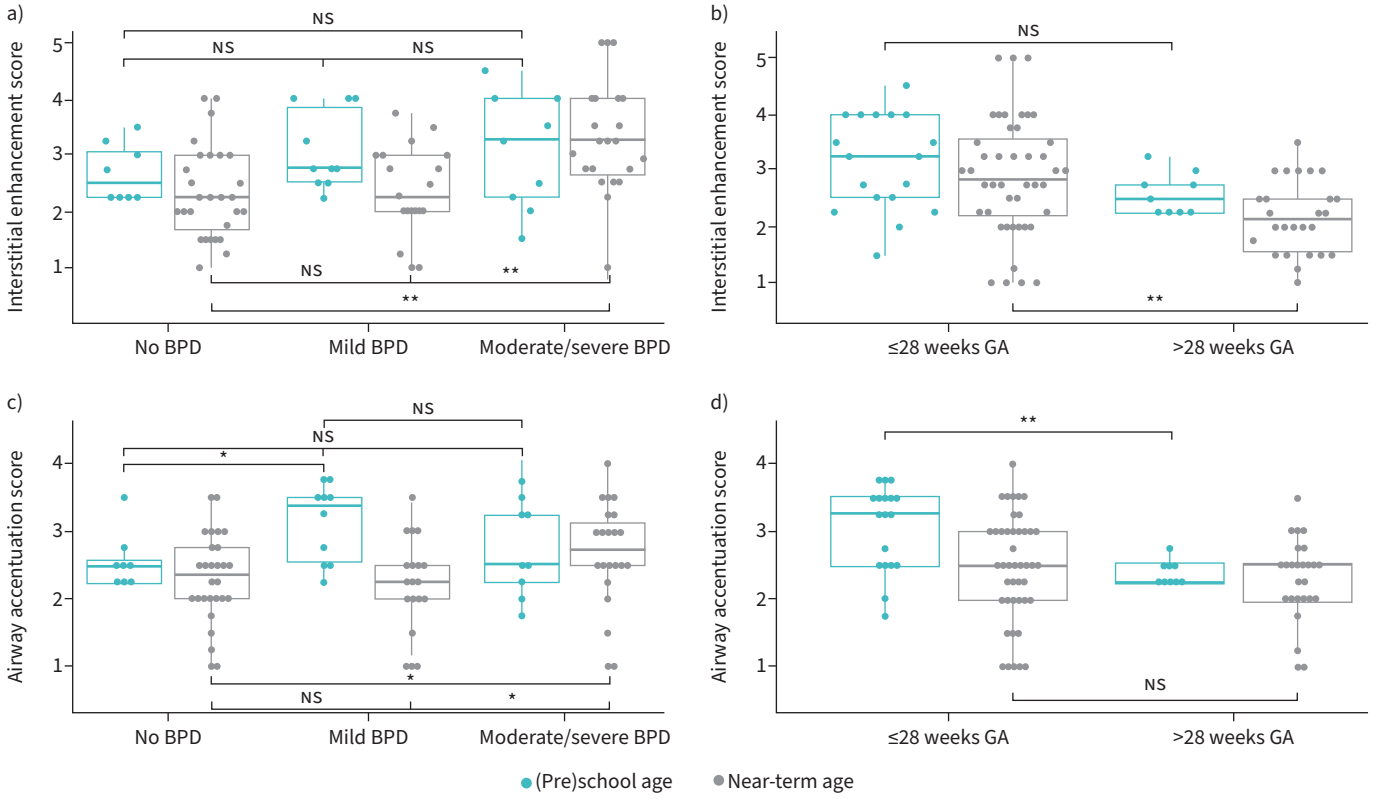

FIGURE 3 a) Assessment of "interstitial enhancement" in infants with moderate/severe bronchopulmonary dysplasia (BPD) at (pre)school and near-term age when compared to infants without or with mild BPD. b) Comparisons for "interstitial enhancement" scores in preterm infants born ⩽28 weeks and >28 weeks gestational age (GA) at (pre)school and at near-term age. c) Assessment of "airway accentuation" in infants with moderate/severe BPD at (pre)school and near-term age when compared to infants without or with mild BPD. d) Comparisons for "airway accentuation scores in preterm infants born ⩽28 weeks and >28 weeks GA at (pre)school and at near-term age. Points indicate individual cases. The MRI score is based on a semi-quantitative 5-point Likert scale, where 1 represents the absence of any abnormality, 5 represents maximum pathology. Median, 25% and 75% quartiles; whiskers represent 1.5 times the interquartile range (IQR). NS: nonsignificant. NS: p>0.05; *: p⩽0.05; **: p⩽0.01. In boxplots, p-values were calculated by Mann–Whitney U-test.

concept allows a cross-sectional view on developmental trajectories in BPD, COPD and asthma, demonstrating that lung function can be tracked along a consistent percentile from infancy to childhood to young adulthood [84]. A relation between BPD and diseases such as COPD [79, 85, 86] is supported by data suggesting that BPD can develop from a predominantly alveolar [48] into an obstructive lung disease, thereby mimicking lung function abnormalities of COPD [87, 88]. The hypothesis for early-in-life events as a critical determinant of lung function in later life [89–91] is reflected by latest COPD definitions [92].

Although dysanaptic growth of the airways is discussed as an underlying mechanism [79, 85, 89], in preterms likely influenced by corticosteroid administration, ventilator therapy and oxygen supplementation [93–95], the concept still lacks deeper insight into (shared) pathogenetic mechanisms that could describe the complexities of airway–parenchymal interactions and interdependence [80]. We would like to highlight, however, that the comparison with adult diseases holds value for the description of disease phenotypes on a trajectory including outlook on risk scores, monitoring and treatment strategies, while having to avoid oversimplifications as underlying pathophysiology likely includes shared and distinct mechanisms [96–100].

Technically, image acquisition in the high field strength of 3 tesla provided us with an increased signal-to-noise ratio (factor 2 when compared to 1.5 tesla), especially important when imaging infants with low body weight and subsequent small FOVs and corresponding small voxel dimensions. The advantage of T2-weighted fast-spin-echo images includes its reduced susceptibility to effects that can compromise gradient-echo acquisitions of the lung parenchyma at 3 tesla. Short scan times minimise the influence of movement while adapting the sequences to the physiological conditions of our patients with higher heart and respiratory rates. Basing our scoring approach on optimised standard pulse sequences (single-shot fast

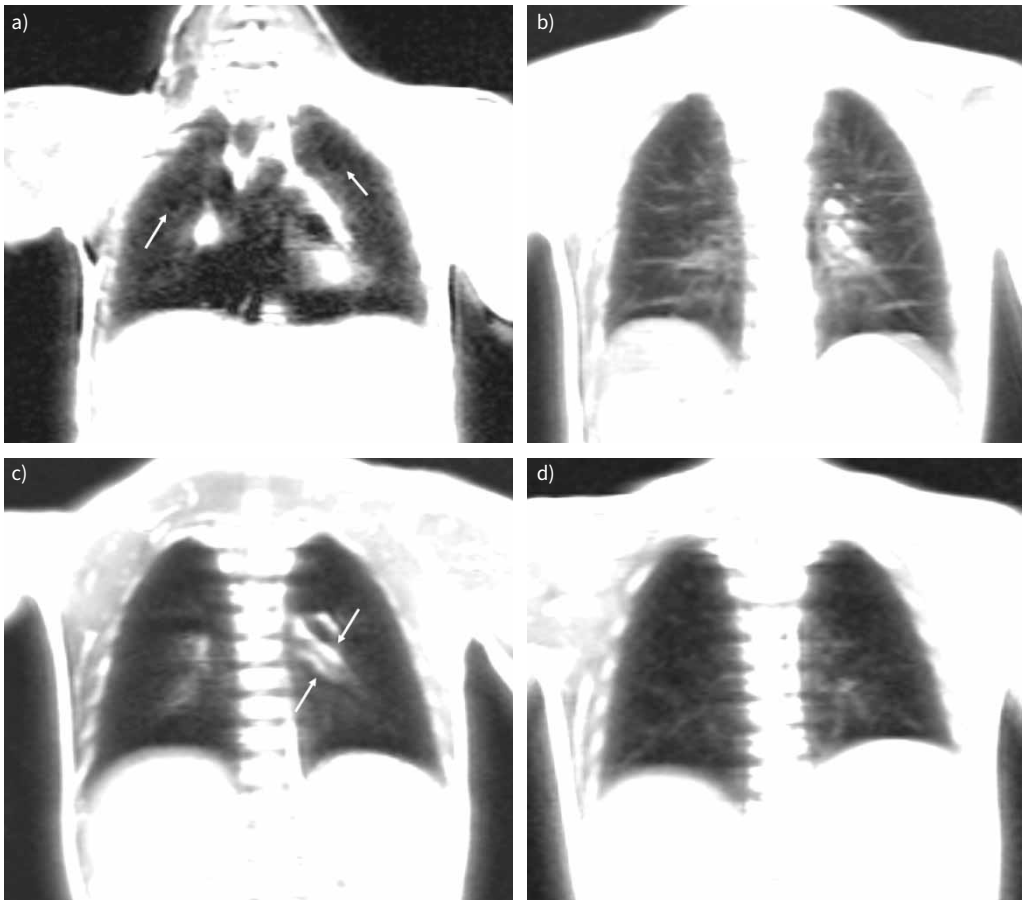

FIGURE 4 Magnetic resonance imaging (MRI) scoring system for the semiquantitative assessment of structural disease characteristics in preterm infants with bronchopulmonary dysplasia (BPD). Representative lung MRIs of infants in coronal planes at (pre)school age: a) example of an "emphysema" score of 4; b) example of an interstitial enhancement score of 4.5; c) example of an accentuated airway score of 4; and d) a reference scan with low values for all lung morphologies. Arrows in part a indicate bullae and reduced signal intensity; arrows in part c indicate increased airway signal and airway thickness. Definition of the MRI score variables "emphysema" (reduced signal intensity, rarefied lung vasculature, hyperexpansion, mosaic pattern of lung attenuation, bullae or blebs), "interstitial enhancement" (distinctive representation of intestinal structures, thickening of bronchovascular bundle), "airway accentuation" (increased signal intensity in the respiratory ducts, airway wall thickness in relation to airway). Scoring is achieved by the means of a five-point Likert scale with 1 reflecting physiological result and 5 referring to maximum pathology. The variables are assessed for each of the four lung quadrants separately.

spin echo) ensures general availability at clinical 3-tesla scanners. For future applications, a promising field in paediatric imaging is that of functional MRI [101] with the possibility of combining structural and functional analysis indicating pulmonary ventilation and perfusion without the need for ionising radiation or contrast agents [102]. As of today, this method is highly specialised and, in contrast to our protocol [33], reserved for only a few centres, hindering its broad application. Likewise, the promising technology of low-field, high-resolution MRI using a field strength of 0.55 likely bears benefits for the paediatric population as it shows advantages for any structure in the body that moves or is near air such as the heart as well as the lungs [103]. However, its use is currently restricted to only selected paediatric studies, pending a final assessment of its value and comparability.

Future studies with increased cohort sizes that follow a longitudinal design and include term-born children as a second control group need to address the important impact of sex as well as continuous exposure to airborne pollutants on lung function in later life [47, 90, 104].

In summary, our results emphasize the importance of diagnostic tools to capture trajectories of (adverse) pulmonary development [100, 105] stemming from the disruption of alveolar differentiation [105]. Adding to the very few studies addressing the structural nature of dysanapsis, our study provides important insight into structural changes in the potential framework of this concept, with the predominance of tissue rarefication and overdistension in an emphysema-like pattern persisting from the neonatal period [84] into preschool age depending on the degree of immaturity. Studies are needed to evaluate current concepts of disease prevention and treatment in this context reaching from antenatal steroid therapy, surfactant and methylxanthines [106] to strategies avoiding lung damage inflicted by invasive respiratory support and high oxygen supplementation [58] or the treatment of arising complications [58, 106], all the way to the ultimate use of lung volume reduction in end-stage BPD cases [107–109].

The use of a clinically applicable scoring system to identify structural changes can enable harmonised postnatal and follow-up imaging strategies. Our MRI scans are therefore balanced to display MRI images with the highest possible resolution and contrast under the conditions relevant in paediatric radiology, while the choice of sequences (single-shot T2-weighted turbo-spin-echo sequences in contrast to newer UTE or ZTE techniques) allows for their application in different centres and settings through low-threshold accessibility, further supported by the web-based application [33].

In conclusion, a close network of neonatologists, paediatricians and adult pulmonologists is needed to provide adequate care for patients with BPD throughout life where, in best case scenarios, structural assessments are partnered with biomarkers from liquid biopsies [110] to improve monitoring strategies further.

Acknowledgement: We sincerely thank our AIRR patients and their families for their invaluable contribution to the study.

Provenance: Submitted article, peer reviewed

Support statement: The present study was supported by the Young Investigator Grant NWG VH-NG-829 by the Helmholtz Foundation and the Helmholtz Zentrum Muenchen, Germany, the German Centre for Lung Research (DZL) (BMBF)), the transregional collaborative research centre PILOT (TRR 359 Perinatal Development of Immune Cell Topology) of the university of Freiburg and the LMU Munich, and the Research Training Group “Targets in Toxicology” (GRK2338) of the German Science and Research Organisation (DFG). Additional financial support was provided by the Stiftung AtemWeg (LSS AIRR). Helmholtz Zentrum München; DOI: https://dx.doi.org/10.13039/501100013295; Deutsches Zentrum für Lungenforschung; DOI: https://dx.doi.org/10.13039/501100010564; Stiftung Atemweg; Deutsche Forschungsgemeinschaft; DOI: https://dx.doi.org/10.13039/501100001659.

This trial is registered with the German Registry for Clinical Studies, identifier number DRKS00004600.

Ethics approval: An ethics vote was required as this is an observational study on humans: EC #195-07, Ethic Board of the Ludwig-Maximilians University.

Author contributions: Conception and design of the manuscript was done by AH. The data were acquired by KS, DS, KF. Data analysis and interpretation were performed by AH, AK, KF, KS. The manuscript was written by AH, KF, KS, AK. Literature research was done by AH, KF and KS, figures were done by AH, AK, OD and KF. The manuscript was drafted for important intellectual content and reviewed by AH, AK, KS, OD, SS, FH, BS, FH, AWF and KF.

Conflict of interest: A. Hilgendorff reports support for the present manuscript from Young Invesigator Grant NWG, VH-NG-829, Helmholtz Foundation, German Centre for Lung Research (DZL) Institutional funds, Transregional collaborative research center PILOT (TRR 359 Perinatal Development of Immune Cell Topology, DFG), Research Training Group ‘Targets in Toxicology’ (GRK2338) of the German Science and Research Organisation (DFG) and Stiftung AtemWeg (LSS AIRR); Consultancy fees from Chiesi GmbH; payment or honoraria for lectures, presentations, speakers bureaus, manuscript writing or educational events for Thieme Publishing and Chiesi; support received for attending meetings from FASEB Conference and GPP Meeting; patents planned, issued or pending for WO 2018/091665; participation on a Data Safety Monitoring Board or Advisory Board for BOW, EU Advisory Board and CPC-M bioArchive. D. Steffinger reports support for the present manuscript from LMU University Hospital, LMU Munich, Munich, Germany (contract as an MRI technician). O. Dietrich reports grants from Siemens Healthineers, Erlangen, Germany. F. Heinen reports a leadership role with the Neuropaediatric Society. S. Stöcklein reports payment or honoraria for lectures, presentations, speakers bureaus, manuscript writing or educational events from Siemens, Bayer and Philips; participation on a Data Safety Monitoring Board or Advisory Board for Bayer AG. The remaining authors have nothing to disclose.

References

1 Glass HC, Costarino AT, Stayer SA, *et al.* Outcomes for extremely premature infants. *Anesth Analg* 2015; 120: 1337–1351.
2 Osterman MJK, Hamilton BE, Martin JA, *et al.* Births: final data for 2021. *Natl Vital Stat Rep* 2023; 72: 1–53.
3 Yannekis G, Passarella M, Lorch S. Differential effects of delivery hospital on mortality and morbidity in minority premature and low birth weight neonates. *J Perinatol* 2020; 40: 404–411.
4 Petrova A, Mehta R, Anwar M, *et al.* Impact of race and ethnicity on the outcome of preterm infants below 32 weeks gestation. *J Perinatol* 2003; 23: 404–408.
5 Ancel P-Y, Goffinet F, EPIPAGE-2 Writing Group, *et al.* Survival and morbidity of preterm children born at 22 through 34 weeks' gestation in France in 2011: results of the EPIPAGE-2 cohort study. *JAMA Pediatr* 2015; 169: 230–238.
6 Stoll BJ, Hansen NI, Bell EF, *et al.* Trends in care practices, morbidity, and mortality of extremely preterm neonates, 1993-2012. *JAMA* 2015; 314: 1039–1051.
7 Jobe AH, Bancalari E. Bronchopulmonary dysplasia. *Am J Respir Crit Care Med* 2001; 163: 1723–1729.
8 Jensen EA, Schmidt B. Epidemiology of bronchopulmonary dysplasia. *Birth Defects Res A Clin Mol Teratol* 2014; 100: 145–157.
9 Baker CD, Alvira CM. Disrupted lung development and bronchopulmonary dysplasia: opportunities for lung repair and regeneration. *Curr Opin Pediatr* 2014; 26: 306–314.
10 Bui DS, Perret JL, Walters EH, *et al.* Association between very to moderate preterm births, lung function deficits, and COPD at age 53 years: analysis of a prospective cohort study. *Lancet Respir Med* 2022; 10: 478–484.
11 Di Filippo P, Dodi G, Ciarelli F, *et al.* Lifelong lung sequelae of prematurity. *Int J Environ Res Public Health* 2022; 19: 5273.
12 Fawke J, Lum S, Kirkby J, *et al.* Lung function and respiratory symptoms at 11 years in children born extremely preterm: the EPICure study. *Am J Respir Crit Care Med* 2010; 182: 237–245.
13 Carr H, Cnattingius S, Granath F, *et al.* Preterm birth and risk of heart failure up to early adulthood. *J Am Coll Cardiol* 2017; 69: 2634–2642.
14 Crump C, Groves A, Sundquist J, *et al.* Association of preterm birth with long-term risk of heart failure into adulthood. *JAMA Pediatr* 2021; 175: 689–697.
15 May C, Prendergast M, Salman S, *et al.* Chest radiograph thoracic areas and lung volumes in infants developing bronchopulmonary dysplasia. *Pediatr Pulmonol* 2009; 44: 80–85.
16 Fitzgerald DA, Van Asperen PP, Lam AH, *et al.* Chest radiograph abnormalities in very low birthweight survivors of chronic neonatal lung disease. *J Paediatr Child Health* 1996; 32: 491–494.
17 Greenough A, Kavvadia V, Johnson AH, *et al.* A simple chest radiograph score to predict chronic lung disease in prematurely born infants. *Br J Radiol* 1999; 72: 530–533.
18 Yuksel B, Greenough A, Karani J, *et al.* Chest radiograph scoring system for use in pre-term infants. *Br J Radiol* 1991; 64: 1015–1018.
19 Kubota J, Ohki Y, Inoue T, *et al.* Ultrafast CT scoring system for assessing bronchopulmonary dysplasia: reproducibility and clinical correlation. *Radiat Med* 1998; 16: 167–174.
20 Ochiai M, Hikino S, Yabuuchi H, *et al.* A new scoring system for computed tomography of the chest for assessing the clinical status of bronchopulmonary dysplasia. *J Pediatr* 2008; 152: 90–95, 95.
21 Oppenheim C, Mamou-Mani T, Sayegh N, *et al.* Bronchopulmonary dysplasia: value of CT in identifying pulmonary sequelae. *AJR Am J Roentgenol* 1994; 163: 169–172.
22 Shin S-M, Kim WS, Cheon J-E, *et al.* Bronchopulmonary dysplasia: new high resolution computed tomography scoring system and correlation between the high resolution computed tomography score and clinical severity. *Korean J Radiol* 2013; 14: 350–360.
23 Higano NS, Spielberg DR, Fleck RJ, *et al.* Neonatal pulmonary magnetic resonance imaging of bronchopulmonary dysplasia predicts short-term clinical outcomes. *Am J Respir Crit Care Med* 2018; 198: 1302–1311.
24 Walkup LL, Tkach JA, Higano NS, *et al.* Quantitative magnetic resonance imaging of bronchopulmonary dysplasia in the neonatal intensive care unit environment. *Am J Respir Crit Care Med* 2015; 192: 1215–1222.
25 Hahn AD, Higano NS, Walkup LL, *et al.* Pulmonary MRI of neonates in the intensive care unit using 3D ultrashort echo time and a small footprint MRI system. *J Magn Reson Imaging* 2017; 45: 463–471.
26 Oda K, Ishimoto H, Yatera K, *et al.* High-resolution CT scoring system-based grading scale predicts the clinical outcomes in patients with idiopathic pulmonary fibrosis. *Respir Res* 2014; 15: 10.
27 Sileo C, Corvol H, Boelle P-Y, *et al.* HRCT and MRI of the lung in children with cystic fibrosis: comparison of different scoring systems. *J Cyst Fibros* 2014; 13: 198–204.
28 Tulek B, Kivrak AS, Ozbek S, *et al.* Phenotyping of chronic obstructive pulmonary disease using the modified Bhalla scoring system for high-resolution computed tomography. *Can Respir J* 2013; 20: 91–96.
29 Förster K, Sass S, Ehrhardt H, *et al.* Early identification of bronchopulmonary dysplasia using novel biomarkers by proteomic screening. *Am J Respir Crit Care Med* 2018; 197: 1076–1080.

30 Couchard M, Polge J, Bomsel F. Hyaline membrane disease: diagnosis, radiologic surveillance, treatment and complications. *Ann Radiol (Paris)* 1974; 17: 669–683.
31 Franz AR, Steinbach G, Kron M, *et al.* Interleukin-8: a valuable tool to restrict antibiotic therapy in newborn infants. *Acta Paediatr* 2001; 90: 1025–1032.
32 Sherman MP, Goetzman BW, Ahlfors CE, *et al.* Tracheal aspiration and its clinical correlates in the diagnosis of congenital pneumonia. *Pediatrics* 1980; 65: 258–263.
33 Förster K, Marchi H, Stöcklein S, *et al.* Magnetic resonance imaging-based scoring of the diseased lung in the preterm infant with bronchopulmonary dysplasia: UNiforme Scoring of the disEAsed Lung in BPD (UNSEAL BPD). *Am J Physiol Lung Cell Mol Physiol* 2023; 324: L114–L122.
34 Eichinger M, Optazaite D-E, Kopp-Schneider A, *et al.* Morphologic and functional scoring of cystic fibrosis lung disease using MRI. *Eur J Radiol* 2012; 81: 1321–1329.
35 Likert R. A technique for the measurement of attitudes. *Arch Psychol* 1932; 140: 1–55.
36 Förster K, Ertl-Wagner B, Ehrhardt H, *et al.* Altered relaxation times in MRI indicate bronchopulmonary dysplasia. *Thorax* 2020; 75: 184–187.
37 Cutillo AG, Chan PH, Ailion DC, *et al.* Characterization of bleomycin lung injury by nuclear magnetic resonance: correlation between NMR relaxation times and lung water and collagen content. *Magn Reson Med* 2002; 47: 246–256.
38 Stadler A, Stiebellehner L, Jakob PM, *et al.* Quantitative and o(2) enhanced MRI of the pathologic lung: findings in emphysema, fibrosis, and cystic fibrosis. *Int J Biomed Imaging* 2007; 2007: 23624.
39 Yi CA, Lee KS, Han J, *et al.* 3-T MRI for differentiating inflammation- and fibrosis-predominant lesions of usual and nonspecific interstitial pneumonia: comparison study with pathologic correlation. *AJR Am J Roentgenol* 2008; 190: 878–885.
40 Broström EB, Thunqvist P, Adenfelt G, *et al.* Obstructive lung disease in children with mild to severe BPD. *Respir Med* 2010; 104: 362–370.
41 Aukland SM, Rosendahl K, Owens CM, *et al.* Neonatal bronchopulmonary dysplasia predicts abnormal pulmonary HRCT scans in long-term survivors of extreme preterm birth. *Thorax* 2009; 64: 405–410.
42 Narayanan M, Beardsmore CS, Owers-Bradley J, *et al.* Catch-up alveolarization in ex-preterm children: evidence from (3)He magnetic resonance. *Am J Respir Crit Care Med* 2013; 187: 1104–1109.
43 Simpson SJ, Logie KM, O'Dea CA, *et al.* Altered lung structure and function in mid-childhood survivors of very preterm birth. *Thorax* 2017; 72: 702–711.
44 Simpson SJ, Turkovic L, Wilson AC, *et al.* Lung function trajectories throughout childhood in survivors of very preterm birth: a longitudinal cohort study. *Lancet Child Adolesc Health* 2018; 2: 350–359.
45 Flors L, Mugler JP 3rd, Paget-Brown A, *et al.* Hyperpolarized helium-3 diffusion-weighted magnetic resonance imaging detects abnormalities of lung structure in children with bronchopulmonary dysplasia. *J Thorac Imaging* 2017; 32: 323–332.
46 Simpson SJ, Hallberg J, PELICAN Clinical Research Collaboration, *et al.* The PELICAN (Prematurity's Effect on the Lungs In Children and Adults Network) ERS Clinical Research Collaboration: understanding the impact of preterm birth on lung health throughout life. *Eur Respir J* 2021; 57: 2004387.
47 Lundberg B, Merid SK, Um-Bergström P, *et al.* Lung function in young adulthood in relation to moderate-to-late preterm birth. *ERJ Open Res* 2024; 10: 00701-2023.
48 Coalson JJ. Pathology of bronchopulmonary dysplasia. *Semin Perinatol* 2006; 30: 179–184.
49 Spielberg DR, Walkup LL, Stein JM, *et al.* Quantitative CT scans of lung parenchymal pathology in premature infants ages 0-6 years. *Pediatr Pulmonol* 2018; 53: 316–323.
50 Sung T-J, Hwang SM, Kim MY, *et al.* Relationship between clinical severity of 'new' bronchopulmonary dysplasia and HRCT abnormalities in VLBW infants. *Pediatr Pulmonol* 2018; 53: 1391–1398.
51 Boechat MCB, de Mello RR, da Silva KS, *et al.* A computed tomography scoring system to assess pulmonary disease among premature infants. *Sao Paulo Med J* 2010; 128: 328–335.
52 Hentschel R, Jorch G (eds). 1 Embryologie der Lungenentwicklung. In: Fetoneonatale Lunge. Stuttgart, Georg Thieme Verlag, 2017; pp. 22–29.
53 Collins JJP, Tibboel D, de Kleer IM, *et al.* The future of bronchopulmonary dysplasia: emerging pathophysiological concepts and potential new avenues of treatment. *Front Med* 2017; 4: 61.
54 Hartling L, Liang Y, Lacaze-Masmonteil T. Chorioamnionitis as a risk factor for bronchopulmonary dysplasia: a systematic review and meta-analysis. *Arch Dis Child Fetal Neonatal Ed* 2012; 97: F8–F17.
55 Bhandari V, Bizzarro MJ, Shetty A, *et al.* Familial and genetic susceptibility to major neonatal morbidities in preterm twins. *Pediatrics* 2006; 117: 1901–1906.
56 Lavoie PM, Pham C, Jang KL. Heritability of bronchopulmonary dysplasia, defined according to the consensus statement of the National Institutes of Health. *Pediatrics* 2008; 122: 479–485.
57 Parker RA, Lindstrom DP, Cotton RB. Evidence from twin study implies possible genetic susceptibility to bronchopulmonary dysplasia. *Semin Perinatol* 1996; 20: 206–209.
58 Thébaud B, Goss KN, Laughon M, *et al.* Bronchopulmonary dysplasia. *Nat Rev Dis Primers* 2019; 5: 78.

59 Moschino L, Bonadies L, Baraldi E. Lung growth and pulmonary function after prematurity and bronchopulmonary dysplasia. *Pediatr Pulmonol* 2021; 56: 3499–3508.
60 Bårdsen T, Røksund OD, Benestad MR, *et al.* Tracking of lung function from 10 to 35 years after being born extremely preterm or with extremely low birth weight. *Thorax* 2022; 77: 790–798.
61 Chan JYC, Stern DA, Guerra S, *et al.* Pneumonia in childhood and impaired lung function in adults: a longitudinal study. *Pediatrics* 2015; 135: 607–616.
62 Postma DS, Bush A, van den Berge M. Risk factors and early origins of chronic obstructive pulmonary disease. *Lancet* 2015; 385: 899–909.
63 Duijts L, Jaddoe VWV, van der Valk RJP, *et al.* Fetal exposure to maternal and paternal smoking and the risks of wheezing in preschool children: the Generation R Study. *Chest* 2012; 141: 876–885.
64 Morrow LA, Wagner BD, Ingram DA, *et al.* Antenatal determinants of bronchopulmonary dysplasia and late respiratory disease in preterm infants. *Am J Respir Crit Care Med* 2017; 196: 364–374.
65 Berger J, Bhandari V. Animal models of bronchopulmonary dysplasia. The term mouse models. *Am J Physiol Lung Cell Mol Physiol* 2014; 307: L936–L947.
66 McGrath-Morrow SA, Lauer T, Collaco JM, *et al.* Neonatal hyperoxia contributes additively to cigarette smoke-induced chronic obstructive pulmonary disease changes in adult mice. *Am J Respir Cell Mol Biol* 2011; 45: 610–616.
67 Krishnan JK, Martinez FJ. Lung function trajectories and chronic obstructive pulmonary disease: current understanding and knowledge gaps. *Curr Opin Pulm Med* 2018; 24: 124–129.
68 Vanhaverbeke K, Van Eyck A, Van Hoorenbeeck K, *et al.* Lung imaging in bronchopulmonary dysplasia: a systematic review. *Respir Med* 2020; 171: 106101.
69 Bentsen MH, Markestad T, Øymar K, *et al.* Lung function at term in extremely preterm-born infants: a regional prospective cohort study. *BMJ Open* 2017; 7: e016868.
70 Proietti E, Riedel T, Fuchs O, *et al.* Can infant lung function predict respiratory morbidity during the first year of life in preterm infants? *Eur Respir J* 2014; 43: 1642–1651.
71 Robin B, Kim Y-J, Huth J, *et al.* Pulmonary function in bronchopulmonary dysplasia. *Pediatr Pulmonol* 2004; 37: 236–242.
72 Ronkainen E, Dunder T, Peltoniemi O, *et al.* New BPD predicts lung function at school age: follow-up study and meta-analysis. *Pediatr Pulmonol* 2015; 50: 1090–1098.
73 Simpson SJ, Hall GL, Wilson AC. Lung function following very preterm birth in the era of 'new' bronchopulmonary dysplasia. *Respirology* 2015; 20: 535–540.
74 Urs R, Kotecha S, Hall GL, *et al.* Persistent and progressive long-term lung disease in survivors of preterm birth. *Paediatr Respir Rev* 2018; 28: 87–94.
75 Duke JW, Lewandowski AJ, Abman SH, *et al.* Physiological aspects of cardiopulmonary dysanapsis on exercise in adults born preterm. *J Physiol* 2022; 600: 463–482.
76 Balinotti JE, Chakr VC, Tiller C, *et al.* Growth of lung parenchyma in infants and toddlers with chronic lung disease of infancy. *Am J Respir Crit Care Med* 2010; 181: 1093–1097.
77 Margraf LR, Tomashefski JF Jr, Bruce MC, *et al.* Morphometric analysis of the lung in bronchopulmonary dysplasia. *Am Rev Respir Dis* 1991; 143: 391–400.
78 Islam JY, Keller RL, Aschner JL, *et al.* Understanding the short- and long-term respiratory outcomes of prematurity and bronchopulmonary dysplasia. *Am J Respir Crit Care Med* 2015; 192: 134–156.
79 Cousins M, Hart K, Kotecha SJ, *et al.* Characterising airway obstructive, dysanaptic and PRISm phenotypes of prematurity-associated lung disease. *Thorax* 2023; 78: 895–903.
80 McGinn EA, Mandell EW, Smith BJ, *et al.* Dysanapsis as a determinant of lung function in development and disease. *Am J Respir Crit Care Med* 2023; 208: 956–963.
81 Chan H-F, Smith LJ, Biancardi AM, *et al.* Image phenotyping of preterm-born children using hyperpolarized Xe lung magnetic resonance imaging and multiple-breath washout. *Am J Respir Crit Care Med* 2023; 207: 89–100.
82 Stern DA, Morgan WJ, Wright AL, *et al.* Poor airway function in early infancy and lung function by age 22 years: a non-selective longitudinal cohort study. *Lancet* 2007; 370: 758–764.
83 Bush A. How early do airway inflammation and remodeling occur? *Allergol Int* 2008; 57: 11–19.
84 Bush A. COPD: a pediatric disease. *COPD* 2008; 5: 53–67.
85 Mochizuki F, Tanabe N, Shimada T, *et al.* Centrilobular emphysema and airway dysanapsis: factors associated with low respiratory function in younger smokers. *ERJ Open Res* 2024; 10: 00695-2023.
86 McGrath-Morrow SA, Collaco JM. Bronchopulmonary dysplasia: what are its links to COPD? *Ther Adv Respir Dis* 2019; 13: 1753466619892492.
87 GBD 2015 Chronic Respiratory Disease Collaborators. Global, regional, and national deaths, prevalence, disability-adjusted life years, and years lived with disability for chronic obstructive pulmonary disease and asthma, 1990-2015: a systematic analysis for the Global Burden of Disease Study 2015. *Lancet Respir Med* 2017; 5: 691–706.
88 Jobe AH, Bancalari E. An all-inclusive perspective on bronchopulmonary dysplasia. *J Pediatr* 2021; 234: 257–259.

89 Markopoulou P, Papanikolaou E, Analytis A, *et al.* Preterm birth as a risk factor for metabolic syndrome and cardiovascular disease in adult life: a systematic review and meta-analysis. *J Pediatr* 2019; 210: 69–80.

90 Goulden N, Cousins M, Hart K, *et al.* Inhaled corticosteroids alone and in combination with long-acting β2 receptor agonists to treat reduced lung function in preterm-born children: a randomized clinical trial. *JAMA Pediatr* 2022; 176: 133–141.

91 Barker DJ, Godfrey KM, Fall C, *et al.* Relation of birth weight and childhood respiratory infection to adult lung function and death from chronic obstructive airways disease. *BMJ* 1991; 303: 671–675.

92 Caramori G, Casolari P, Barczyk A, *et al.* COPD immunopathology. *Semin Immunopathol* 2016; 38: 497–515.

93 Klinger G, Levy I, Sirota L, *et al.* Outcome of early-onset sepsis in a national cohort of very low birth weight infants. *Pediatrics* 2010; 125: e736–e740.

94 Lahra MM, Beeby PJ, Jeffery HE. Intrauterine inflammation, neonatal sepsis, and chronic lung disease: a 13-year hospital cohort study. *Pediatrics* 2009; 123: 1314–1319.

95 Schlapbach LJ, Aebischer M, Adams M, *et al.* Impact of sepsis on neurodevelopmental outcome in a Swiss National Cohort of extremely premature infants. *Pediatrics* 2011; 128: e348–e357.

96 Doyle LW. Evaluation of neonatal intensive care for extremely-low-birth-weight infants. *Semin Fetal Neonatal Med* 2006; 11: 139–145.

97 Baraldi E, Filippone M. Chronic lung disease after premature birth. *N Engl J Med* 2007; 357: 1946–1955.

98 Bourbon JR, Boucherat O, Boczkowski J, *et al.* Bronchopulmonary dysplasia and emphysema: in search of common therapeutic targets. *Trends Mol Med* 2009; 15: 169–179.

99 Fortis S, Georgopoulos D, Tzanakis N, *et al.* Chronic obstructive pulmonary disease (COPD) and COPD-like phenotypes. *Front Med (Lausanne)* 2024; 11: 1375457.

100 Nissen G, Hinsenbrock S, Rausch TK, *et al.* Lung function of preterm children parsed by a polygenic risk score for adult COPD. *NEJM Evid* 2023; 2: EVIDoa2200279.

101 Campbell-Washburn AE, Malayeri AA, Jones EC, *et al.* T2-weighted lung imaging using a 0.55-T MRI system. *Radiol Cardiothorac Imaging* 2021; 3: e200611.

102 Ilicak E, Thater G, Ozdemir S, *et al.* Functional lung imaging of 2-year-old children after congenital diaphragmatic hernia repair using dynamic mode decomposition MRI. *Eur Radiol* 2024; 34: 3761–3772.

103 Arnold TC, Freeman CW, Litt B, *et al.* Low-field MRI: clinical promise and challenges. *J Magn Reson Imaging* 2023; 57: 25–44.

104 Majewska R, Pac A, Mróz E, *et al.* Lung function growth trajectories in non-asthmatic children aged 4–9 in relation to prenatal exposure to airborne particulate matter and polycyclic aromatic hydrocarbons: Krakow birth cohort study. *Environ Res* 2018; 166: 150–157.

105 Simpson SJ, Du Berry C, Evans DJ, *et al.* Unravelling the respiratory health path across the lifespan for survivors of preterm birth. *Lancet Respir Med* 2024; 12: 167–180.

106 Álvarez-Fuente M, Moreno L, Mitchell JA, *et al.* Preventing bronchopulmonary dysplasia: new tools for an old challenge. *Pediatr Res* 2019; 85: 432–441.

107 Willers C, Maager L, Bauman G, *et al.* School-age structural and functional MRI and lung function in children following lung resection for congenital lung malformation in infancy. *Pediatr Radiol* 2022; 52: 1255–1265.

108 Sohn B, Park S, Park IK, *et al.* Lung volume reduction surgery for respiratory failure in infants with bronchopulmonary dysplasia. *Pediatrics* 2018; 141: S395–S398.

109 Allen J, Zwerdling R, Ehrenkranz R, *et al.* Statement on the care of the child with chronic lung disease of infancy and childhood. *Am J Respir Crit Care Med* 2003; 168: 356–396.

110 Harris SL, Troughton R, Lewis L, *et al.* Circulating forms of B-type natriuretic peptide in very preterm infants. *J Appl Lab Med* 2020; 5: 506–515.